

DESIGN OF A PDA-BASED STETHOSCOPE FOR
PULMONARY SOUND PARAMETRIZATION AND
CLASSIFICATION

by

Ömer Faruk Özdemir

B.S. in E.E., Boğaziçi University, 2007

Submitted to the Institute for Graduate Studies in
Science and Engineering in partial fulfillment of
the requirements for the degree of
Master of Science

Graduate Program in Electrical and Electronics Engineering
Boğaziçi University

2010

ACKNOWLEDGEMENTS

I am grateful to Prof. Yasemin P. Kahya for giving me a chance to complete this study, for her positive approach in situations where I am stuck, for her kindness and help that gave me courage to complete this study.

I would like to thank İpek Şen, the only member of Lung Acoustic Lab. She was magically present when I needed help. Thank you for your endless support, encouragement, smile and friendship. She was really a key to complete this task.

I'm also grateful to my dear friends Serkan Sayılır and Dursun Baran, for their support, friendship, and encouragement although they are very far away from me. Also, I would like to thank Oğuz Atasoy, for his endless support and friendship.

Last but probably the most important "Thank you" is for my family. Without their love, support, and encouragement, I wouldn't be able to complete this task surely. Their patience and trust at the times I felt hopeless made me get up and finish this work.

ABSTRACT

DESIGN OF A PDA-BASED STETHOSCOPE FOR PULMONARY SOUND PARAMETRIZATION AND CLASSIFICATION

Technological developments made in the near past, gave us a chance to analyze respiratory sounds quantitatively. Digitization of respiratory sounds, obviously, was the key in the analysis of respiratory sounds. Although the stethoscope is still the most practical tool, some of its drawbacks may be eliminated with a digital hand-held tool designed for the same purposes.

In this thesis, a one-channel respiratory sound acquisition and analysis system has been designed and implemented. Respiratory sounds are captured via a microphone placed on the chest wall. They are then amplified and filtered by a hardware system, designed for the purposes of this thesis. Finally, they are digitized and processed in a hand-held device. A user interface program is written to process digitized respiratory sounds in LabVIEW, which classifies the subject as healthy or pathological.

This hand-held device designed as a digital stethoscope eliminates the need of a physician during recording and is very useful as a first stage screening device. Moreover, it records data over a wider bandwidth than that of a stethoscope, where most of the useful information is contained.

ÖZET

AKCİĞER SESLERİNİN PARAMETRELENMESİ VE SINIFLANDIRILMASI İÇİN PDA TABANLI BİR STETOSKOP GELİŞTİRİLMESİ

Yakın geçmişte yapılan teknolojik gelişmeler, bize akciğer seslerinin sayısal olarak analizinin yapılabilmesi olanağını tanıyor. Solunum seslerinin sayısallaştırılması, şüphesiz ki bu seslerin analizinin yapılabilmesinde anahtar bir konumdadır. Stetoskop, hala bu alandaki en pratik alet olsa da, aynı amaç için tasarlanmış bir cep bilgisayarı stetoskobun bazı olumsuz yönlerini ortadan kaldırabilir.

Bu tezde, tek kanallı solunum sesi edinim ve analiz sistemi tasarlanmış ve gerçekleştirilmiştir. Solunum sesleri, sırtta yerleştirilmiş bir mikrofon vasıtasıyla kaydedilmiştir. Daha sonra bu veriler, bir donanım devresi vasıtasıyla yükseltilmiş ve bant geçiren süzgeç ile süzülmüştür. Son olarak da cep bilgisayarı ile sayısallaştırılmış ve işlenmiştir. LabVIEW'da sayısallaştırılmış solunum seslerini işlemek için, kişiyi sağlıklı ya da hasta olarak sınıflandıran bir kullanıcı arayüz programı yazılmıştır.

Dijital stetoskop olarak geliştirilmiş bu cihaz, dinleme sırasında hekime olan ihtiyacı ortadan kaldırır ve ilk adım görüntüleme cihazı olarak çok kullanışlıdır. Ayrıca, bu cihaz, çoğu kullanışlı bilgilerin olduğu, stetoskoptan daha geniş bir aralığı dinleyebilir

TABLE OF CONTENTS

ACKNOWLEDGEMENTS	iii
ABSTRACT	iv
ÖZET	v
LIST OF FIGURES	viii
LIST OF TABLES	xi
LIST OF SYMBOLS/ABBREVIATIONS	xii
1. INTRODUCTION	1
1.1. Respiratory Sounds	2
1.2. Motivation and Aim	3
2. HARDWARE	5
2.1. Microphones and Air Capsules	6
2.2. Amplifier and Filter Unit	8
2.2.1. Instrumentation Amplifier	9
2.2.2. High-Pass Filter	10
2.2.3. Low-Pass Filter	12
2.2.4. Level Adjuster	12
2.2.5. Frequency Responses	14
2.3. Power	14
2.4. PDA	15
2.5. Digitization Unit	16
3. SOFTWARE AND METHODOLOGY	18
3.1. User Interface	19
3.2. Data Acquisition	21
3.3. Graphical Illustration	23
3.4. Library	23
3.4.1. Power Spectral Density	24
3.4.2. Spectral Leakage	25
3.4.3. Windowing	26
3.4.4. Averaging	28

3.4.5. Library Program	30
3.5. k-NN Classification	32
3.6. Analysis	36
4. RESULTS	37
4.1. Offline Results	38
4.2. Online Results	39
5. CONCLUSION	41
6. FUTURE WORK RECOMMENDATIONS	43
APPENDIX A: TECHINAL DRAWING OF THE MICROPHONE CAPSULE	44
APPENDIX B: MICROPHONE SPECIFICATIONS	45
APPENDIX C: DAQ CARD SPECIFICATIONS	46
REFERENCES	48

LIST OF FIGURES

Figure 1.1. An example of early stethoscopes	1
Figure 1.2. Block diagram of the overall system	3
Figure 2.1. A picture of complete hardware	6
Figure 2.2. Drawing of the microphone	6
Figure 2.3. The microphone locations	7
Figure 2.4. Block Diagram of Amplifier and Filter Unit	8
Figure 2.5. A picture of Amplifier and Filter part	9
Figure 2.6. Unity-gain HP KRC filter	10
Figure 2.7. The equal-component LP KRC filter	13
Figure 2.8. Frequency Response of the Amplifier and Filter Unit	14
Figure 2.9. HP iPAQ 2790 EU PDA	15
Figure 2.10. NI CF-6004	16
Figure 2.11. NI CF-6004 Installation	16
Figure 3.1. An example that shows how front panel and block diagram look like, respectively	19

Figure B.1. Microphone specifications	45
Figure C.1. Specifications of DAQ card	46

LIST OF TABLES

Table 2.1. Q and normalized f0 values for 6th order Bessel LPF	11
Table 2.2. Resistor values for HPF	11
Table 2.3. Current consumption of ICs used in the system	15
Table 3.1. k-NN success rate of different averaging numbers for 25 percent overlap and k=5	30
Table 3.2. k-NN classification success rates of the library for various window sizes for k=5, 25 percent overlap	35
Table 3.3. k-NN classification success rates of the library for various k and overlap values	36
Table 4.1. Offline and online results for different “k” and “overlap” values for “window size=2048” and “averaging=15”	37
Table 4.2. Offline results	39
Table 4.3. Online results	40
Table C.1. Terminal Assignments	47
Table C.2. Signal Descriptions	48

LIST OF SYMBOLS/ABBREVIATIONS

CMRR	Common mode rejection ratio
DAQ	Data acquisition
HP	High-pass
HPF	High-pass filter
IA	Instrumentation amplifier
k-NN	k-Nearest Neighbor
LabVIEW	Laboratory Virtual Instrumentation Engineering Workbench
LP	Low-pass
LPF	Low-pass filter
PSD	Power Spectral Density
PC	Personal computer
PCB	Printed circuit board
PDA	Personal digital assistant
RAM	Random-access memory
SMD	Surface mount device
VI	Virtual instrument

1. INTRODUCTION

Auscultation of respiratory sounds has a crucial role since ancient times in medicine. Findings show that Hippocrates advised “immediate auscultation” which is the application of the ear to the patient’s chest. [1] In 1816, René Théophile Hyacinthe Laënnec invented stethoscope, which is combination of Greek words “*stéthos*-chest” and “*skopé*-examination”. The first stethoscope was a simple narrow tube, with a rolled stack of paper. When pressed one end to the patient’s chest, he was able to listen more than “immediate auscultation” from the other end. Thereafter, it had lots of improvements and took its present form. Since its invention, it became the most widely used tool of a physician and never lost popularity.



Figure 1.1. An example of early stethoscopes

Inherent design of stethoscopes is such that they amplify frequencies below 112 Hz and attenuate higher frequencies. Amplification at low frequencies is to be able to hear heart sounds. However, human ear is not very sensitive to sounds at these frequencies. [2]

The respiration-related sound heard on the chest of a healthy person is called normal lung sound. It is like a noise that peaks at frequencies below 100 Hz. At these low frequencies, respiratory sounds are mixed with heart and muscle sounds. Energy of respiratory sounds decrease rapidly at frequencies between 100-200 Hz. [1] The upper level goes to 2000 Hz and 6000 Hz for normal and adventitious respiratory sounds respectively. [3]

Considering the characteristics of respiratory sounds and stethoscopes, the drawbacks of stethoscopes may be summarized as follows. Firstly, auscultation via stethoscope is subjective and depends highly on physician's experience and hearing capability. Moreover, human ear is not very sensitive to lower frequencies despite the fact that, most of energy lies at these frequencies. Furthermore, graphical illustration and saving records is not possible with a stethoscope. Moreover, pathological pulmonary sounds extend well beyond the frequency range of the stethoscopes, thus are attenuated to a great extent.

So, most of these disadvantages may be eliminated by using a "digital" stethoscope. This "digital" stethoscope captures respiratory sounds via a microphone which has a much wider frequency range, and filters them via a hardware system. Filtered data is digitized and analyzed via a PDA. Therefore, this "digital" stethoscope makes it possible to save, to graph and to analyze respiratory data of patients. Subjectivity of stethoscope is also eliminated with this device.

1.1. Respiratory Sounds

Respiratory sounds are considered to be produced by turbulent air flow in trachea. Sounds heard on the chest wall, depend primarily on characteristics of chest wall and filtering effect of lung tissue. The chest wall tends to show low-pass filtering effects and therefore sounds transmitted from the proximal airways are mostly of low frequencies. So, high frequency components of pulmonary sounds have low energy, but contain valuable information for the detection of underlying pathology. [1]

Abnormal respiratory sounds consist of either absent or reduced intensity normal respiratory sounds, exaggerated or excessively loud but otherwise normal respiratory sounds, pathological (bronchial) respiratory sounds, and adventitious sounds - additional sounds not normally present. The current terminology of adventitious respiratory sounds is defined as either continuous or discontinuous. [4]

1.2. Motivation and Aim

The aim of this thesis is to design a digital stethoscope that overcomes the disadvantages of an acoustic stethoscope.

A hand-held device, capable of capturing respiratory sounds and making analysis, may make auscultation a much more valuable diagnosis tool. Moreover, it may offer the physicians the opportunity to look and store a graphical illustration of patient's respiratory sounds. Physicians will have a chance to take a look at graphical illustration of patient's respiratory sounds. Therefore, the subjectivity of auscultation via stethoscope may be eliminated. Moreover, the physicians may have a chance to observe respiratory sounds at frequencies where human ear is not very sensitive.

Figure 1.2 shows block diagram of the overall system. Respiratory sounds are captured by an electret microphone, and then amplified and band-pass filtered (constructed with a cascade of a high-pass filter and a low-pass filter). Thereafter, they are digitized by a DAQ card placed on the hand-held device (PDA). Finally, respiratory sounds are displayed, stored and processed by PDA.

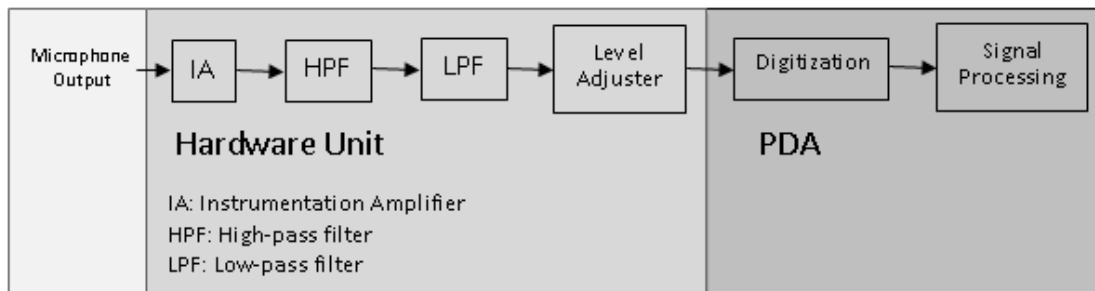


Figure 1.2. Block diagram of the overall system

A user interface program has been written, to process digitized data. It displays graphical illustration of respiratory sounds of subjects and analyzes them. It can record respiratory data of subjects and make a decision whether the subject is healthy or not with some accuracy.

Such a small hand-held device, designed as a digital stethoscope, offers new opportunities in medicine. It can be used at homes as a pre-diagnosis tool so that people will have a chance to regularly control their breath sounds without any need a physician. Or it can be used in small towns or rural areas where it is hard to get an advanced treatment, as a pre-diagnosis tool.

The algorithm running on the device lets the subjects know whether their lungs are pathological or not. However, it can be improved to accomplish more tasks as recording patients' respiratory sounds and replaying them. The scope of the thesis is to demonstrate that a digital hand-held device that is capable of capturing, processing, and analyzing respiratory sounds is achievable.

2. HARDWARE

A hardware card is necessary to capture respiratory sounds, and then amplify and filter captured data, and finally digitize amplified and filtered data to be able to process by a hand-held device.

Respiratory sounds are captured via an electret microphone placed on the chest wall. Captured data are band-pass filtered (a cascade of a high-pass and a low-pass filter) in order to eliminate environment and friction noise, muscle and heart sounds. Thereafter, filtered data are amplified since they are small in magnitude. Finally, they are digitized by a DAQ card which is placed on a hand-held device (PDA). Digitization is necessary to be able to process respiratory sounds on a PDA.

Hardware card (Amplifier and filter unit) design belongs to the Master Thesis of İpek Şen. [6] Nevertheless, for a complete understanding of this work, all hardware units will be explained in detail.

Hardware unit can be divided into 4 parts as follows:

- i. Microphones and air capsules
- ii. Amplifier and filter unit
- iii. Digitization unit
- iv. PDA

A picture of complete hardware can be seen in Figure 2.1.

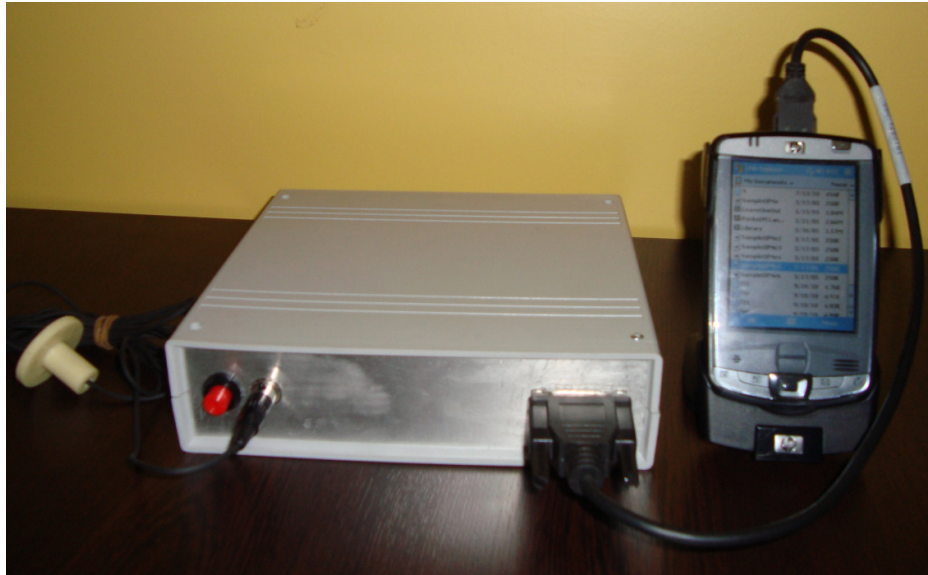


Figure 2.1. A picture of complete hardware

2.1. Microphones and Air Capsules

Respiratory sounds are captured using the Sony ECM-44BPT electret microphone with three leads (5 Volt supply, ground and signal). Figure 2.2 shows a drawing that depicts the cross section of the microphone and air capsule.

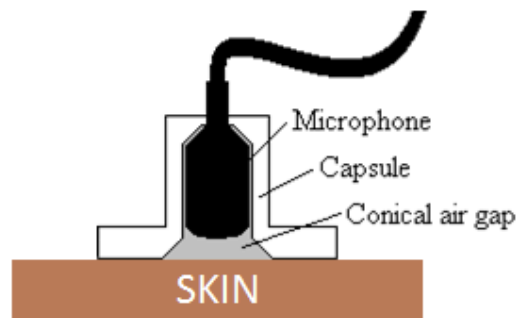


Figure 2.2. Drawing of the microphone [6]

As can be seen from the figure, the design of the microphone is very similar to the design of the stethoscope. There is a conical air gap between microphone and skin which makes respiratory sounds more audible. When coupled to the skin with a capsule [8], similar to a stethoscope bell, this type of microphone is a sensitive lung sound transducer.

This explains why this type of microphone is commonly used in capturing respiratory sounds. Also, these small electret microphones are widely available for speech and music recording. [2]

For microphone locations, a detailed study has been conducted by İpek Şen with the guidance of a physician specialized in pulmonary medicine in her master thesis, and this valuable information is used. In order for a complete understanding, the work has been mentioned here. The microphone distributions are shown in Figure 2.3.

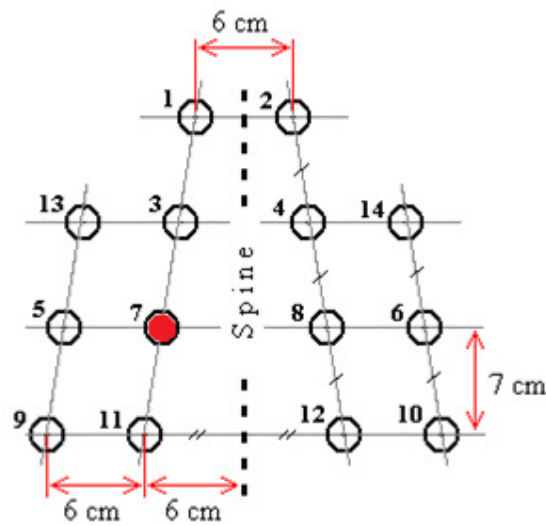


Figure 2.3. The microphone locations [6]

The distribution of microphones scans all of the chest wall. However, since the designed system consists of one channel, one location among 14 should be selected. Location shown as “7” in the figure, is the best place to obtain the flow as has been shown in a study conducted in our laboratory. Therefore, if one location has to be selected among 14, the location numbered as “7” is the best.

The technical drawing of the microphone is given in Appendix A and its specifications are given in Appendix B.

2.2. Amplifier and Filter Unit

This unit takes lung sounds from a microphone, filters and amplifies, and then sends them to the DAQ card to be digitized. One microphone forms a respiratory channel which consists of an instrumentation amplifier, a high-pass filter, a low-pass filter and a level adjuster [6]. Apart from respiratory channels, there is a voltage regulator part.

Normal lung sounds tend to occur at frequencies between 37.5 and 1000 Hz. Some of the energy lies at frequencies below 100 Hz. The heart and muscle sounds also occur at frequencies below 100 Hz, so they are mixed up at these frequencies. [1] Therefore, there is a need to filter frequencies below 100 Hz. Most researches show that a filtering with cut-off frequency in the range of 30-150 Hz should be applied to eliminate heart and muscle sounds. [5] Also, another filtering with cut-off frequency in the range of 1600-3000 Hz should be applied for anti-aliasing. Block diagram of the Amplifier and Filter unit can be seen in Figure 2.4.

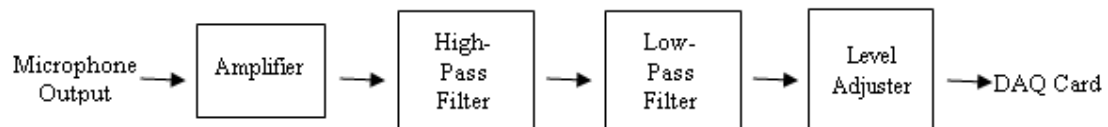


Figure 2.4. Block Diagram of Amplifier and Filter Unit

Figure 2.5 shows a picture of PCB. As mentioned above, this PCB is designed for a 14 channel pulmonary sound data acquisition along with flow data. However, one channel data acquisition without flow control is implemented in this work. Therefore, flow part shown in the picture is not used and only one unit among four is used in IA and LPF part. Also, cut-off frequency of LPF is adjusted to 2000 Hz.

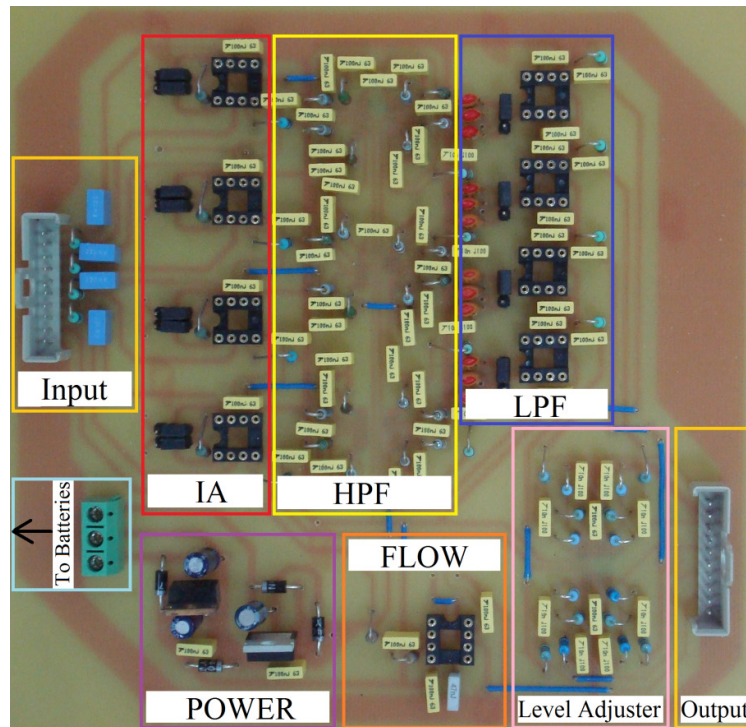


Figure 2.5. A picture of Amplifier and Filter part

2.2.1. Instrumentation Amplifier

An instrumentation amplifier is a difference amplifier which has following characteristics:

- Low noise,
- High CMRR,
- Accurate and stable gain,

INA128 (Burr-Brown) has been chosen which is a low-power and precision instrumentation amplifier. It has wide supply range which changes from ± 2.25 to ± 18 V with a low quiescent current of $700 \mu\text{A}$. It has a maximum offset voltage of $50 \mu\text{V}$, a maximum drift of $0,5 \mu\text{V}/^\circ\text{C}$, a minimum CMRR of 120 dB and input protection up to ± 40 V. It has also an adjustable gain of which can be calculated as follows:

$$G = 1 + \frac{50 \text{ k}\Omega}{R_G} \quad (2.1)$$

2.2.2. High-Pass Filter

The low frequency environment and friction noise and muscle and heart sounds exist and need to be filtered from the recorded lung sounds. Researches show that cut-off frequency of the high-pass filter should be somewhere between 30 and 150 Hz and pass-band ripples should not be allowed [5]. Researches also suggest to use linear phase response and to have a skirt slope should be greater than 18 dB/oct [9]. These requirements are best achieved with a 6th order Bessel filter which results a slope of 36 dB/oct in the reject-band. The cut-off frequency is chosen to be 80 Hz.

The 6th order HP Bessel filter is implemented with 3 cascaded unity-gain HP KRC filters. The unity-gain HP KRC filter can be shown in Figure 2.6 and equations for HP KRC filters are given below.

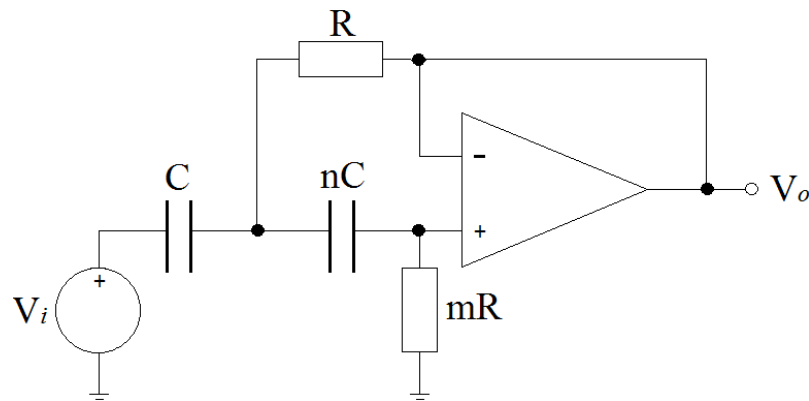


Figure 2.6. Unity-gain HP KRC filter [7]

$$f_0 = \frac{1}{2\pi RC\sqrt{mn}} \quad (2.2)$$

$$Q = \frac{\sqrt{mn}}{n+1} \quad (2.3)$$

Normalized f and Q values for the 6th order LP Bessel filter are given in Table 2.1.

Table 2.1. Q and normalized f0 values for 6th order Bessel LPF [7]

f ₀₁	Q ₁	f ₀₂	Q ₂	f ₀₃	Q ₃
1.606	0.510	1.691	0.611	1.907	1.023

To obtain cut-off frequencies of a HPF, the equation given below is used:

$$f_0 = \frac{f_c}{f_{0(\text{table})}} \quad (2.4)$$

where f_c is the cut-off frequency of the overall filter and f_0 is the cut-off frequency of one stage. Using this equation, Q and f values of 3 stages of 6th order Bessel HPF can be obtained easily. Setting $n=1$ and $C=100$ nF and using equations 2.2 and 2.3, following resistance values given in Table 2.2 are calculated [6].

Table 2.2. Resistor values for HPF [6]

	m	R (kΩ)	mR (kΩ)
Stage 1	4.2	18.5 (18.7)	77.7 (76.8)
Stage 2	1.5	27.5 (27.4)	41.25 (41.2)
Stage 3	~1	32 (32.4)	32 (32.4)

MC33204, low-voltage rail-to-rail operational amplifiers are used to implement 6th order Bessel HPF. They offer low noise, high output current capability and a wide common mode input voltage range even with low supply voltages. They have 70 dB CMRR value at 1 kHz and supply voltage of them ranges from ± 0.9 V to ± 6 V.

2.2.3. Low-Pass Filter

To prevent aliasing, LP filtering is needed. Researches indicate that cut-off frequency of LPF should be somewhere between 1600 and 3000 Hz [10]. Higher frequency values may also be chosen to include more details. Moreover, pass-band ripples are not allowed and minimum skirt slope should be 24 dB/oct [9]. So, an 8th order Butterworth filter seems to be suitable to meet these requirements with a 46 dB/oct slope in the reject band [5].

MAX295, an 8th order Butterworth LPF with adjustable cut-off frequency is used. The cut-off frequency can be determined both externally and internally. Internal oscillator is chosen to be clock source of cut-off frequency to prevent noise problems caused by external clock generation. The cut-off frequency of filter can be calculated as follows:

$$f_0 = \frac{f_{osc}}{50} \quad (2.5)$$

where f_{osc} is

$$f_{osc}(\text{kHz}) = \frac{10^5}{3C_{osc}(\text{pF})} \quad (2.6)$$

where C_{osc} is an external capacitor that should be connected to CLK pin of MAX295 to set cut-off frequency. To make it a flexible design, two different cut-off frequency values are chosen, 2000 and 4000 Hz resulting in the choice of 330 and 165 pF, respectively. With a jumper, desired cut-off frequency selection can be made.

According to Nyquist Theorem, cut-off frequency of LPF should be below half of the sampling frequency. So, sampling rate should be at least 4000 Hz.

2.2.4. Level Adjuster

MAX295 used as an 8th order Butterworth LPF is a switched-capacitor filter, therefore its output should be smoothed. In addition, a final gain stage is also needed

since the gain of the preamplifier is not made very high to prevent the saturation of IA by heart and muscle noise. To meet these requirements, an equal-component LP KRC filter ($m=n=1$) is used with a gain of 2 and is depicted in Figure 2.7 [5].

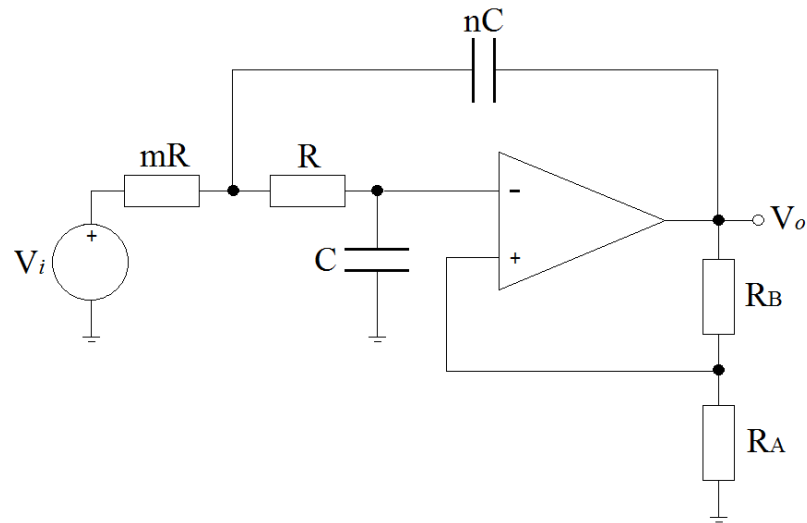


Figure 2.7. The equal-component LP KRC filter ($m=n=1$) [7]

For equal-component case, design equations are

$$f_0 = \frac{1}{2\pi RC} \quad (2.7)$$

$$Q = \frac{1}{3-K} \quad (2.8)$$

$$K = 1 + \frac{R_B}{R_A} \quad (2.9)$$

10 kHz is a good choice for cut-off frequency since it is greater than the cut-off frequency of LPF. Choosing gain to be equal to two results in $R_A=R_B$ (=10 k Ω selected). Then, choosing $C= 10$ nF results in $R= 1.5$ k Ω [6]. Again, MC33204, low-voltage rail-to-rail operational amplifiers are used to build the level adjuster.

2.2.5. Frequency Responses

Cut-off frequencies of a band-pass filter are defined to be the points where output of the filter is -3 dB of the pass-band value. For the hardware that is used to record respiratory sounds, they are 90Hz and 2100 Hz. Frequency response of the hardware can be seen in Figure 2.8.

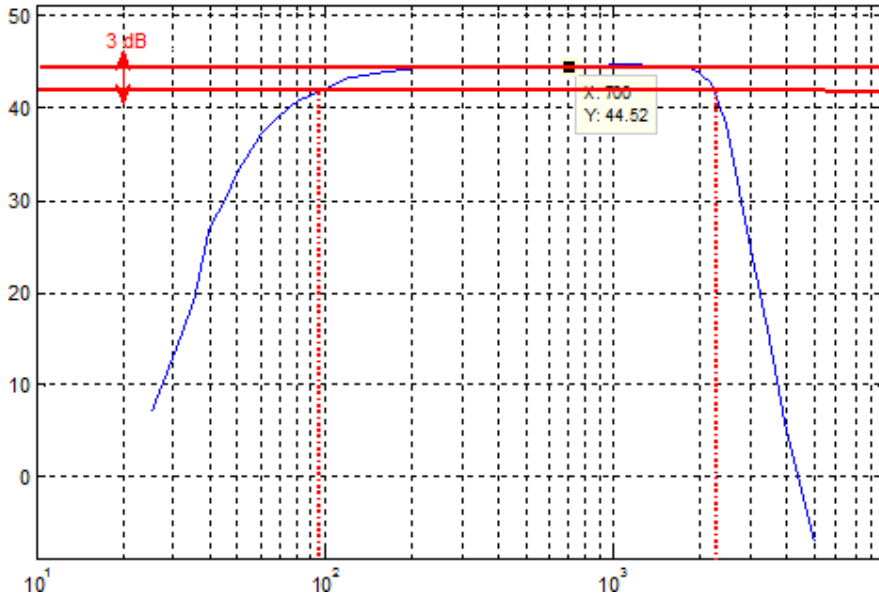


Figure 2.8. Frequency Response of the Amplifier and Filter Unit

2.2.6. Power

The system is powered with ± 12 V supplies. Since MAX295 works only with ± 5 V supplies, ± 12 V is converted to ± 5 V via $\mu A7805$ and $\mu A7905$ voltage regulators.

Typical and maximum current consumption of ICs used in the system are given in Table 2.3. According to these values, power consumption is between 193 mW (typical) and 272.5 mW (maximal).

Table 2.3. Current consumption of ICs used in the system

mA	I _{SUPP} typ.	I _{SUPP} max.
INA128	0.7	0.75
MAX295	15	22
MC33204	0.9 (per amp.)	1.125(per amp.)

2.9. PDA

As a hand-held device, a PDA, HP iPAQ hx2790 EU is used. The hx2790 uses Windows Mobile 5, and it is likely to be the fastest Windows Mobile 5 Pocket PC (2006). It offers a 624 MHz processor, 192 MB of flash ROM for program and file storage, 64 MB RAM, WiFi, Bluetooth, biometric fingerprint security, an SD slot and a CF type II slot. It has a 3.5" TFT touch-screen of resolution 240 x 320.



Figure 2.9. HP iPAQ 2790 EU PDA

Its CF slot enables the user to place a DAQ card for professional applications. In addition, its WiFi feature enables the user to share information on the internet which is a desired feature for professional applications. It gives a chance to share the results of a subject with another doctor or send it to the subject via e-mail.

2.10. Digitization Unit

National Instruments CF-6004 data acquisition (DAQ) device is used for digitization. It has 4 analog, single-ended input channels which have 14 bit ADC resolution and uses successive approximation. It has 200kS/s sampling rate for single channel finite data acquisition, 132 kS/s aggregate sampling rate for multichannel finite data acquisition, 18 kS/s sampling rate for monitoring continuous data acquisition and 1 kS/s sampling rate for graphing continuous data. More information about specifications of DAQ card can be found in the Appendix C.



Figure 2.10. NI CF-6004

This DAQ card is placed on PDA's DAQ card slot as shown in the figure:

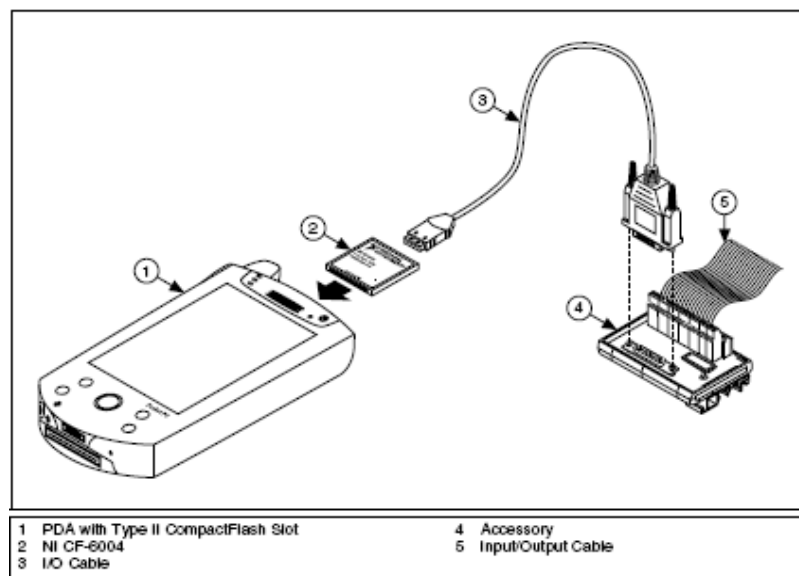


Figure 2.11. NI CF-6004 Installation

Pin diagram of DAQ card can be found in Appendix C, Table C.1 and Table C.2: Only AI GND, AI0 and AI1 pins are used for purposes of the thesis.

DAQ card can be used only with NI LabVIEW PDA software and NI-DAQmx Base software must be installed on NI LabVIEW PDA software for PDA device to be able to recognize DAQ card. For these purposes, NI LabVIEW 8.5 PDA version and NI-DAQmx Base 3.0 version are used.

3. SOFTWARE AND METHODOLOGY

A software program that will run on the PDA is developed to analyze incoming analog respiratory sounds. This program, basically, controls the digitization of analog sounds and provides user interfacing to analyze and process respiratory sounds.

LabVIEW (Laboratory Virtual Instrumentation Engineering Workbench) is a platform and development environment for a visual programming language from National Instruments. LabVIEW which is a commonly used program in signal processing offers a PDA version to accomplish this kind of a task. It has also a DAQ card driver (NI-DAQmx Base is the name used by NI) which gives the user the opportunity to control and analyze analog respiratory sounds. So, combining these 3 software, namely LabVIEW(PC edition), LabVIEW PDA and NI-DAQmx Base, lets the designer to control and digitize respiratory sounds coming from hardware unit, and then process and analyze the data to make a decision on whether the subject is pathological or not by a PDA.

LabVIEW PDA 8.5 is used in this thesis to develop a software program. This PDA version does not have the all functionality that LabVIEW 8.5 provides for PCs. Therefore, it is a limited edition which makes the design more difficult.

The software is installed in the following order: First, LabVIEW 8.5 is installed into a PC, and then PDA extension for LabVIEW 8.5 is installed, and then finally NI-DAQ Base 3.2 is installed for DAQ Card utilities.

All software is created in a PC by using LabVIEW PDA program, and then transferred into a PDA in an executable (.exe) format. Therefore, all codes are created in a PC, no algorithm is developed in PDA.

LabVIEW programs/subroutines are called as VIs (Virtual Instruments) since they imitate real instruments. VIs have 3 parts: the front panel, the block diagram, and the icon/connector. The last is used to represent the VI in the block diagrams of other calling VIs. Figure 3.1 shows how front panel and block diagram look like.

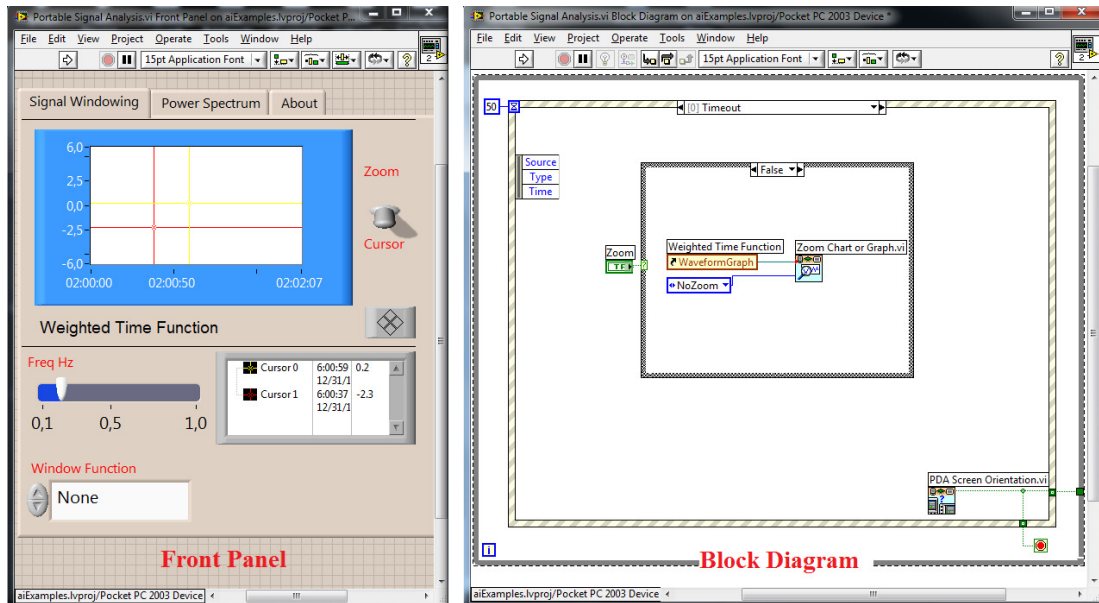


Figure 3.1. An example that shows how front panel and block diagram look like, respectively

3.1. User Interface

A user interface program has been developed for digitization of analog respiratory sounds, and then processing and analyzing digitized data.

The user interface has two tabs one of which is for data acquisition and graphical illustration. The other tab is for data analysis which decides whether the subject is pathological or not.

In the first tab, there are “Start”, “Open”, and “Exit” options. Also, there is “DAQmx Base Task” drop-box to select desired DAQ tasks, “Samples” box which shows how many samples are loaded when pressed to “Open” button, and “Time” box which shows how much time elapsed in seconds since “Start” button is pressed. Figure 3.2 shows how first tab looks like.

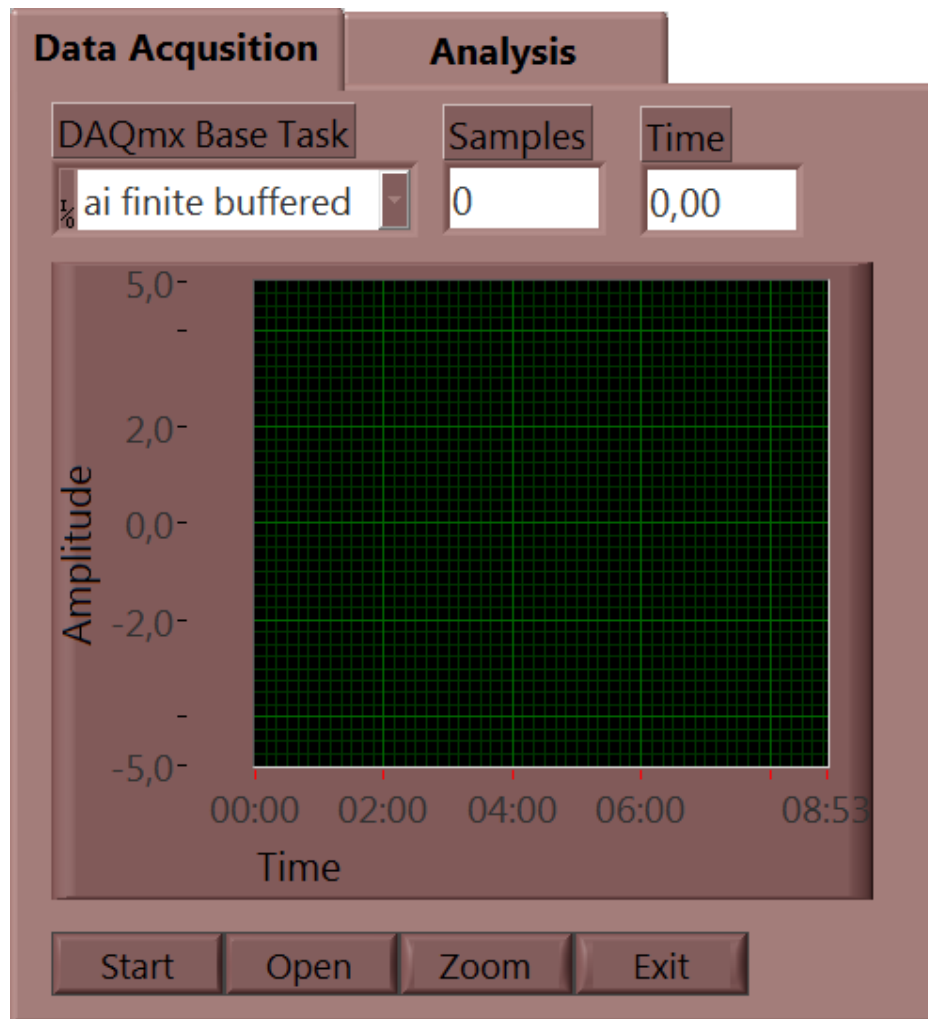


Figure 3.2. User Interface-Data Acquisition Tab

In the second tab, there is “Analyze” option, which analyzes any saved data and compares it with the library to make a decision whether the subject is pathological or not. When the subject is healthy, a small led turns green. Also, there is “Analyzed File” section which shows selected data to be analyzed, “Samples” box which shows how many samples selected data have, “Percentage” box which shows percentage of accuracy of decision. Finally, there are “f25”, “f50”, “f75”, and “f90” arrays which contain quartile frequency data of selected data.

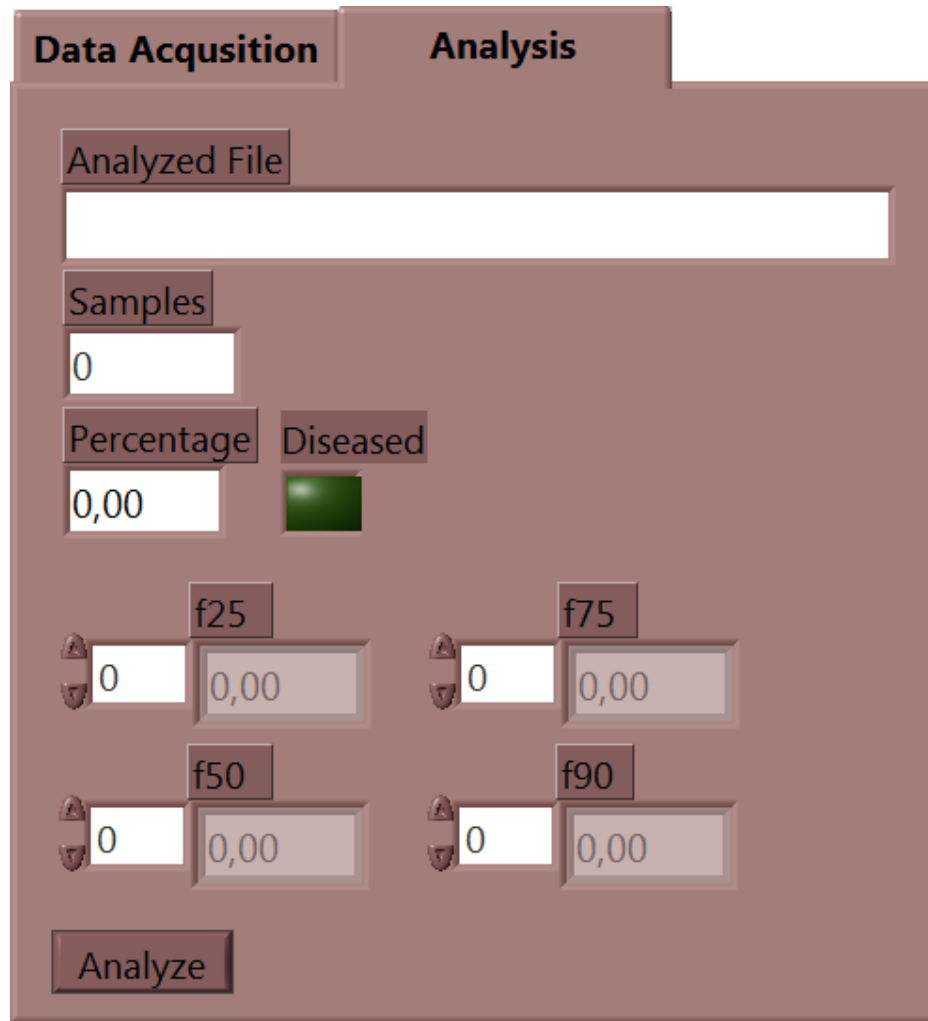


Figure 3.3. User Interface-Analysis Tab

3.2. Data Acquisition

Data acquisition starts when “Start” button is pressed. Data acquisition is accomplished according to the task selected via “DAQmx Base Task” drop-box. The tasks shown in the drop-box are configured under “NI-DAQmx Base Task Configuration Utility” in LabVIEW. Figure 3.3 shows how this section looks like.

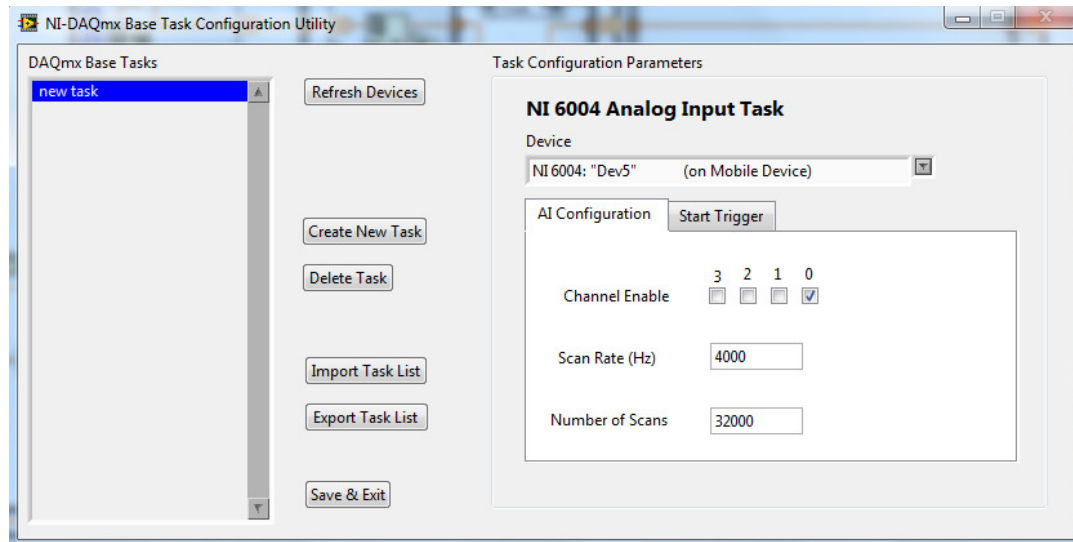


Figure 3.4. NI-DAQmx Base Task Configuration Utility

There are many options that can be configured under this section. Most important ones are “Device” which includes DAQ card models, “Channel Enable” which allows us to enable desired channels, “Scan Rate” which allows us to select desired sample rate, and “Number of Scans” which allows us to select maximum number of samples to acquire. Since hardware unit filters respiratory sound with 2000 Hz, 4000 Hz is selected as “Scan Rate” (Nyquist’s Sampling Theorem) and 32000 as “Number of Scans” since the PDA device can capture 32000 successive samples. Also, NI 6004 is selected from the drop-box since this DAQ card is placed on the PDA device.

Let us look at how data acquisition occurs. When “Start” button is pressed, DAQ Card starts acquiring data from selected channels with selected Scan Rate (Channel 0 and 4000 Hz selected). LabVIEW code builds an array of size 32000 and then asks the user whether to save the data or not. If pressed “OK”, it asks for a name and location for acquired data. It saves the data in “.dat” format which is not a human-readable format but takes up about half the space as compared to text files. If pressed “Cancel”, it discards the array built and is ready for a new data acquisition session.

Although this PDA is one of the best in the market, its low memory limits real time data acquisition. Initial plan was to capture 144000 samples with 9600 Hz, but it is seen that this PDA can only capture 32000 samples with 4000 Hz, successfully. So, cut-off

frequency of LPF is adjusted to 2000 Hz. Also, its low memory prevents real time data illustration impossible. Therefore, the user has to save the real time respiratory sounds first, and then open the saved data and finally have a chance to see how data looks like.

3.3. Graphical Illustration

Graphical illustration unit consists of graphing saved data and zooming into graphed data. Pressing “Open” button, asks for a file name which has a “.dat” extension or full file name like “1.dat” from the user. When the user selects an existing saved data, the data is graphed in the screen. Since, saved data consists of 32000 samples; the graph is adjusted to show 32000 samples only.

Pressing “Zoom” button gives a chance to the user to zoom into desired parts of graphed data. When the user creates a rectangle on the screen of the PDA, that rectangle will be graphed automatically. To return back to the original data, the user should press “Reset Zoom” from “Menu” shortcut.

3.4. Library

In order to make a decision on whether the subject is pathological or not, there should be a library with which to compare the subject’s sound data. Therefore, a new library should be constructed, and new subject’s data should be compared with the data in this library.

Power spectral density analysis of respiratory sounds gives us valuable information. Thus, library will be built upon power spectral density parameters. Fortunately, LabVIEW has a Power Spectral Density VI which has the following properties:

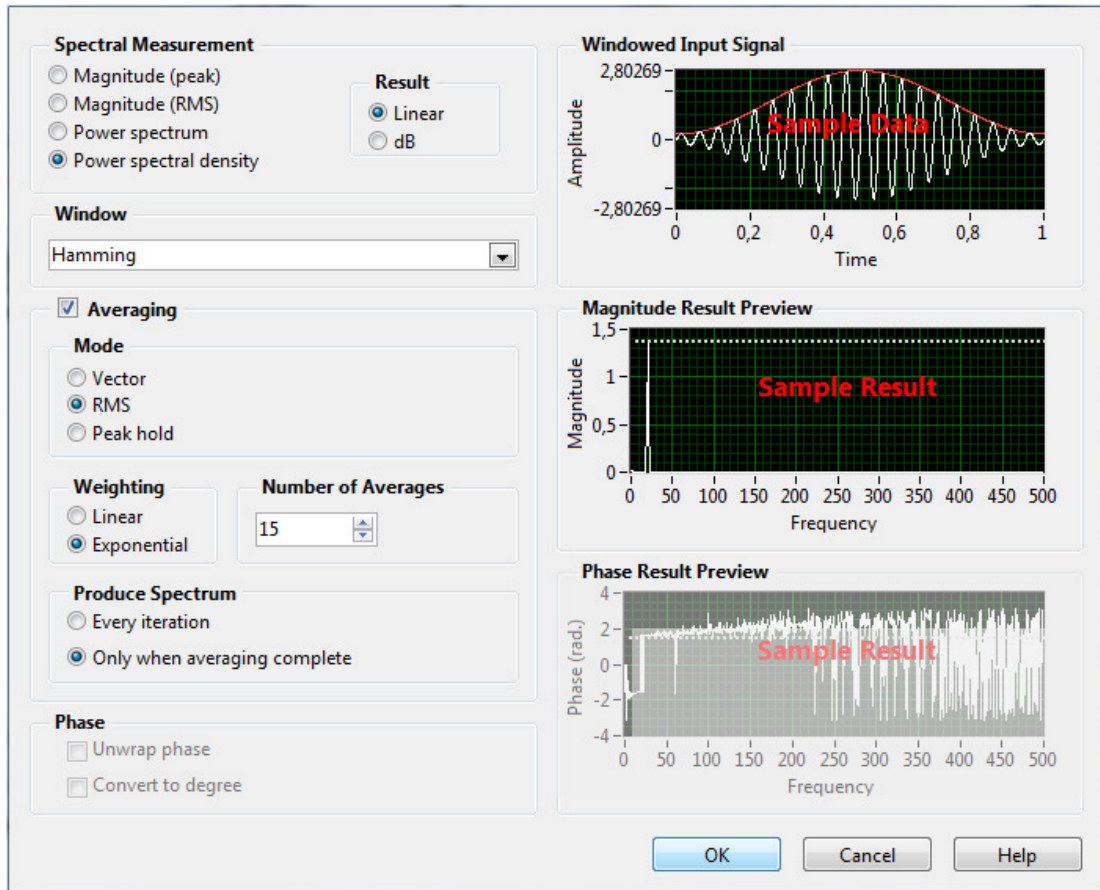


Figure 3.5. Features of Power Spectral Density vi in LabVIEW

3.4.1. Power Spectral Density

Since power spectral density plays an important role, it is critical to understand mathematics behind it.

PSD of a signal defines how the power of that signal is distributed with frequency. It can be formulated as follows:

$$S(f) = \mathcal{F}(\mathcal{R}(\tau)) \quad (3.1)$$

where $\mathcal{F}(x)$ is the fourier transform of “x”, and $\mathcal{R}(y)$ is the autocorrelation function of “y”.

Given a signal $f(t)$, the continuous autocorrelation $R_{ff}(\tau)$ is defined as the continuous cross-correlation integral of $f(t)$ with itself, at lag τ .

$$R_{ff}(\tau) = f^*(-\tau) * f(t) + \int_{-\infty}^{+\infty} f(t + \tau) f^*(t) dt \tag{3.2}$$

where $f^*(x)$ is the complex conjugate of $f(x)$, and “*” represents convolution.[11]

3.4.2. Spectral Leakage

Theoretically, if an infinite time signal is sampled with an infinite set of points, since it is assumed to be periodic, the repetition is smooth at the boundaries. However, in practical applications, there exist finite time signals, and since they are not perfectly periodic, the repetition results in discontinuities at the boundaries. These discontinuities result in leakage of energy from the actual frequency to all other frequencies. This is called “Spectral Leakage”. Figure 3.6 shows an example of waveform with discontinuities.

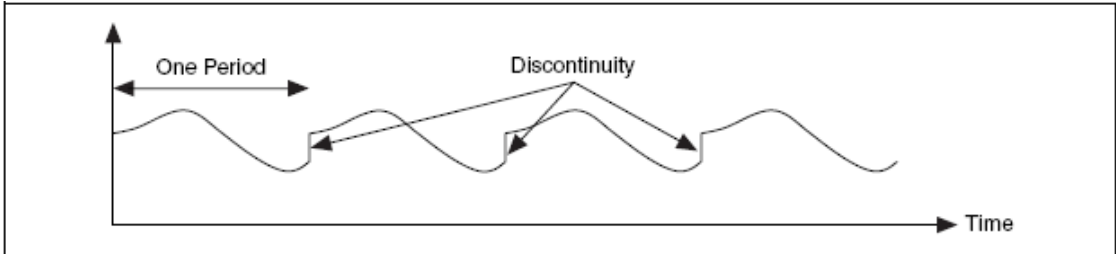


Figure 3.6. Waveform with Discontinuities

A perfect periodic signal in the time record has a spectrum with energy contained in exact frequency bins. A signal that is not periodic in the time record has a spectrum with energy spread across multiple frequency bins. Figure 3.7 shows frequency spectrum of a signal that is not periodic in time domain. As can be seen from the figure, energy of the signal spreads across multiple frequency bins.

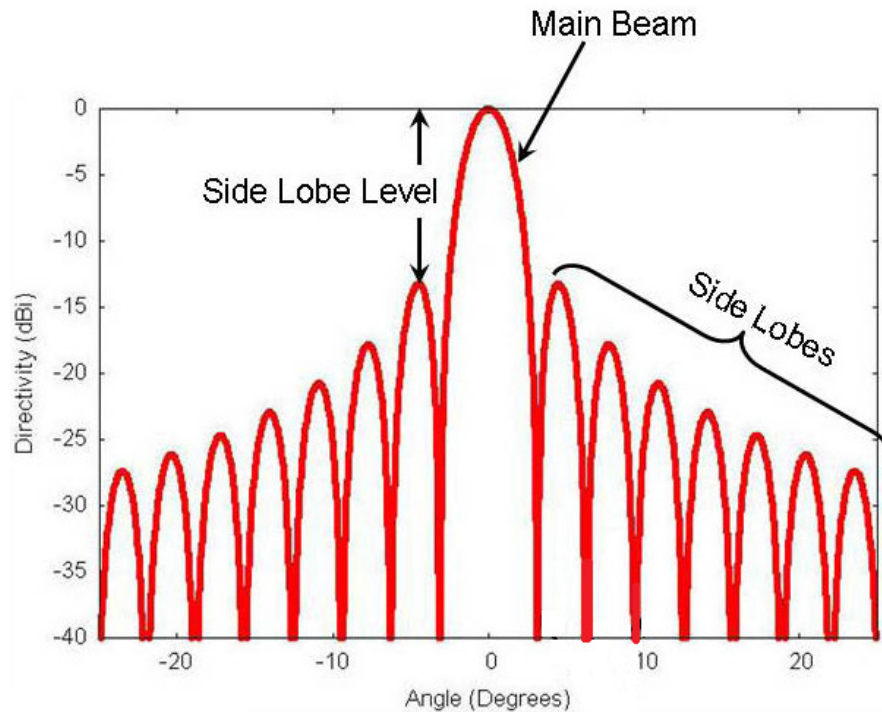


Figure 3.7. Spectral Leakage

3.4.3. Windowing

To overcome spectral leakage, an infinite time record should be taken, from $-\infty$ to $+\infty$. With an infinite time record, the FFT calculates one single line at the correct frequency. However, waiting for infinite time is not possible in practice. To overcome the limitations of a finite time record, windowing is used to reduce the spectral leakage.

The process of windowing a signal involves multiplying the time record by a smoothing window of finite length whose amplitude varies smoothly and gradually towards zero at the edges. The length, or time interval, of a smoothing window is defined in terms of number of samples. Multiplication in the time domain is equivalent to convolution in the frequency domain. Therefore, the spectrum of the windowed signal is a convolution of the spectrum of the original signal with the spectrum of the smoothing window. Windowing changes the shape of the signal in the time domain, as well as affecting the spectrum that results.

Multiplying a signal which is not periodic in time domain, with a window type reduces spectral leakage. Figure 3.8 shows how windowing decreases spectral leakage.

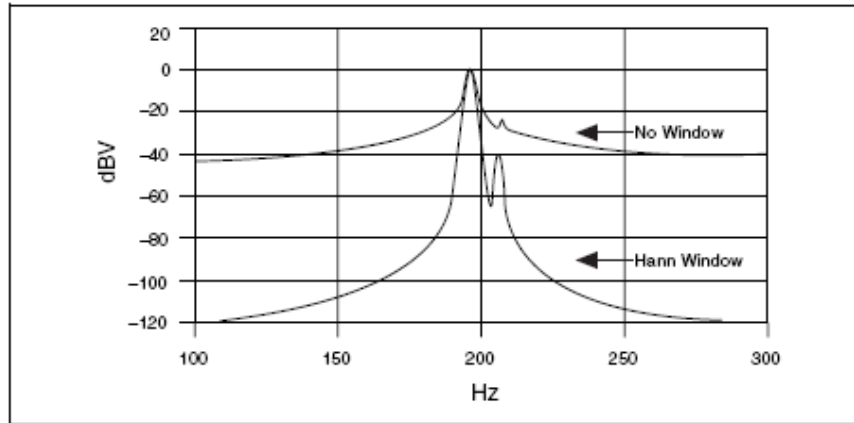


Figure 3.8. Windowing effect on Spectral Leakage

Hamming window is selected as a window type since it is the commonly used window type in spectral measurements of respiratory sounds. Figure 3.9 shows how hamming window looks like in time and frequency domain.

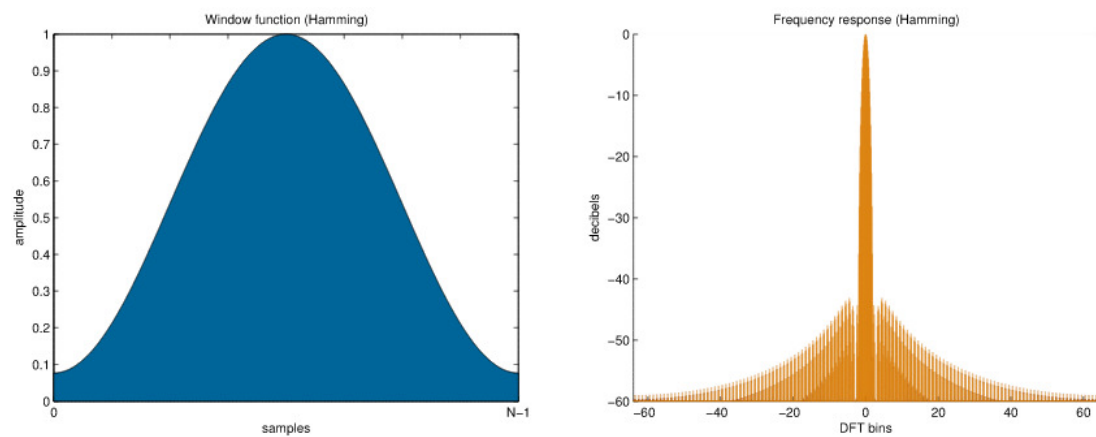


Figure 3.9. Hamming window and its frequency response

The Hamming window is a modified version of the Hanning window. The shape of the Hamming window is similar to that of a cosine wave. The following equation defines the Hamming window.

$$w(n) = 0.54 - 0.46 \cos \frac{2\pi n}{N} \quad (3.3)$$

for $n = 0, 1, 2, \dots, N - 1$ and where N is the length of the window and w is the window value.

Figure 3.10 shows how hamming window looks like in time domain when $N=32$.

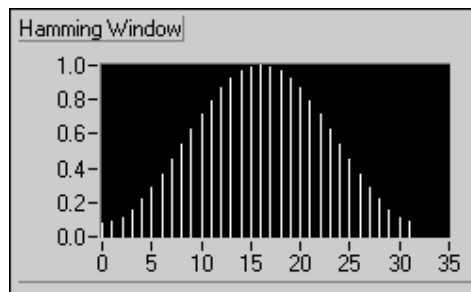


Figure 3.10. Hamming window with $N=32$

3.4.4. Averaging

Averaging successive measurements usually improves measurement accuracy. Averaging usually is performed on measurement results or on individual spectra but not directly on the time record.

You can choose from among the following common averaging modes:

- RMS averaging
- Vector averaging
- Peak hold

RMS averaging reduces signal fluctuations but not the noise floor. The noise floor is not reduced because RMS averaging averages the energy, or power, of the signal. RMS-averaged measurements are computed according to the following equations.

$$\text{Power Spectrum} \quad \langle X^* \cdot X \rangle$$

where X is the complex FFT of signal x (stimulus), X^* is the complex conjugate of X , and $\langle X \rangle$ is the average of X , real and imaginary parts being averaged separately.

Vector averaging eliminates noise from synchronous signals. Vector averaging computes the average of complex quantities directly. The real part is averaged separately from the imaginary part.

$$\text{Power Spectrum} \quad \langle X^* \rangle \cdot \langle X \rangle$$

where X is the complex FFT of signal x (stimulus), X^* is the complex conjugate of X , and $\langle X \rangle$ is the average of X , real and imaginary parts being averaged separately.

Peak hold averaging retains the peak levels of the averaged quantities. Peak hold averaging is performed at each frequency line separately, retaining peak levels from one FFT record to the next.

Power Spectrum

$$\text{MAX}(X^* \cdot X)$$

where X is the complex FFT of signal x (stimulus) and X^* is the complex conjugate of X .

When performing RMS or vector averaging, you can weight each new spectral record using either linear or exponential weighting. Linear weighting combines N spectral records with equal weighting. When the number of averages is completed, the analyzer stops averaging and presents the averaged results. Exponential weighting emphasizes new spectral data more than old and is a continuous process.

Weighting is applied according to the following equation:

$$Y_i = \frac{N-1}{N} Y_{i-1} + \frac{1}{N} X_i \quad (3.4)$$

where X_i is the result of the analysis performed on the i^{th} block, Y_i is the result of the averaging process from X_1 to X_i , $N = i$ for linear weighting, and N is a constant for exponential weighting ($N = 1$ for $i = 1$).

RMS averaging is used in this work, since we are not interested in complex signals and peak levels. Exponential weighting is also used for this work's purposes.

Table 3.1 shows how averaging effects k-NN classifier results. K-NN classifier algorithm will be explained in section 3.6 but this table explains how averaging increases

success rate. Window size is selected to be 2048 samples, and also hamming window type and RMS vector averaging with exponential weighting are used for the test environment.

Table 3.1. k-NN success rate of different averaging numbers for 25 percent overlap and k=5

Window Size	Averaging	Success Rate
2048	No	72.54%
2048	5	76.25%
2048	10	76.87%
2048	15	77.50%
2048	20	76.25%

3.4.5. Library Program

A new LabVIEW program named as “Library.vi” has been created to form a library and the results are also validated with MATLAB program. Library is created using 16 people’s respiratory records, 8 of which are medically diagnosed to be diseased. These records were taken from the data previously obtained in our Lung Acoustics Laboratory. Records were originally taken at a sample rate of 9600 kHz and consisted of 144000 samples. These records are, first, re-sampled at 4000 kHz and then the initial 32000 samples have been taken.

The LabVIEW program that is used to create the library is a very user-friendly one. Figure 3.10 shows how it looks like.

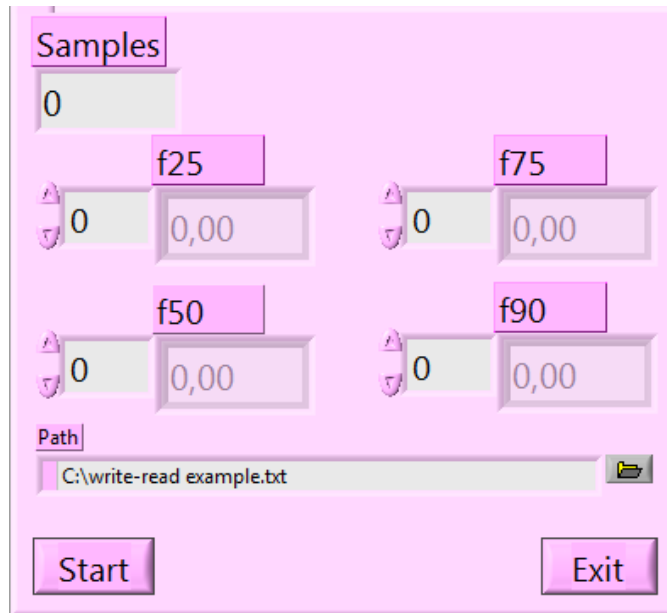


Figure 3.11. Library Program

When “Start” button is pressed, the library program takes a record of a subject who is known to be pathological or healthy by a medical assessment in a text format. Afterwards, the data taken are divided into 20 windows of size 2048, with a 25 percent overlap.

Figure 3.11 shows how 20 windows are created using 32000 samples. Note that 768 samples remain with 20 windows of 25 percent overlap and ignored.

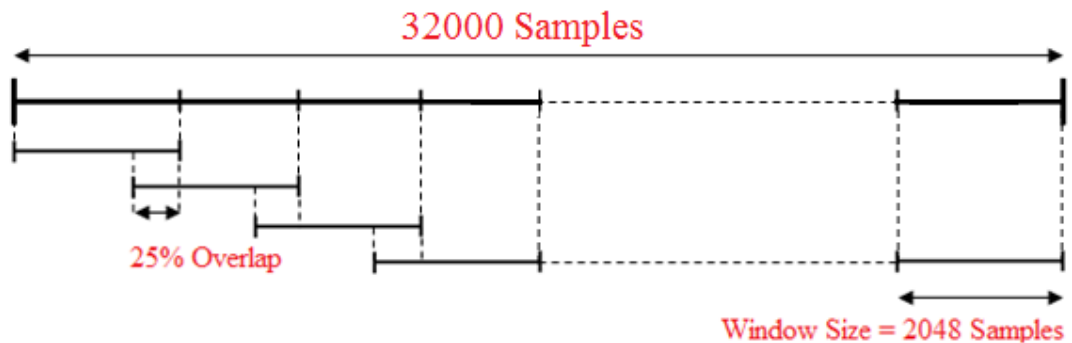


Figure 3.12. Window creation

Then for each window, PSD is calculated and f25, f50, f75, and f90 values are found where “f25” is the frequency where area under PSD graph is 25percent of total area. These frequencies are called “Quartile Frequencies”. Figure 3.12 shows quartile frequencies.

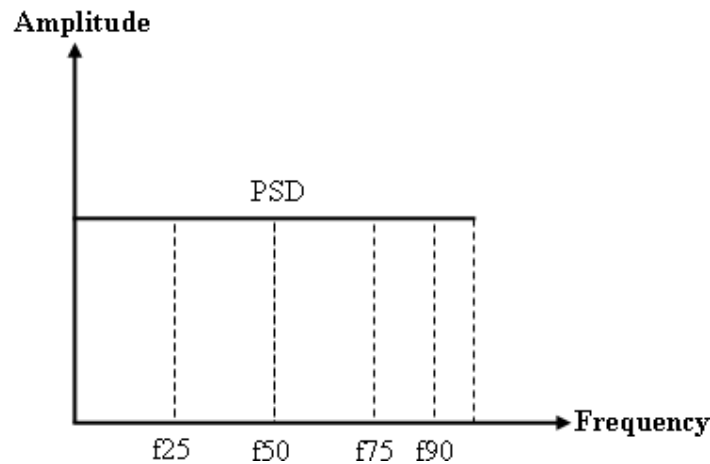


Figure 3.13. Quartile Frequencies

Finally, the results are saved in the text file whose location is given in “Path” part. Quartile frequency results are also given in the screen by f25, f50, f75, and f90 arrays. For each 16 subjects, this program is run once and results are carried into an excel file in a PC manually, to combine all results.

Since there are 20 windows, and 4 frequency values for each window, a vector of size 20 in 4-dimension is created for each record. Therefore, the library consists of a vector of size 320 in 4-dimension whose first 160 values are of healthy subjects and remaining ones are of pathological subjects. So, a new record taken will be compared with this library and a decision will be made accordingly.

3.5. k-NN Classification

In order to train the library, another LabVIEW program is written. This program uses k-NN classification with “leave one out” method to train the library.

In this program, one point (One point in the database has 4 values that correspond to quartile frequencies of a window.) in the library is chosen as an input. Afterwards, “k-

Nearest Neighbor” classification is applied with $k=7$, which means distances to the remaining points in the library is calculated, and then, 7 closest points to the chosen point are decided, and finally, the chosen point is classified as a healthy or pathological one. The closest points to the chosen point are calculated using “Euclidean Distance” method and healthy or pathological classification is done by “Majority Vote”. Then, this decision is compared with actual class of the point since the chosen point is known to be of a healthy or pathological subject. If the result of k -NN classification is the same as the actual class of the chosen point, then this point is known to be classified correctly. After this procedure is applied for all points in the library, overall percentage success rate for all points in the library is calculated. Figure 3.13 summarizes how this method is applied to the library.

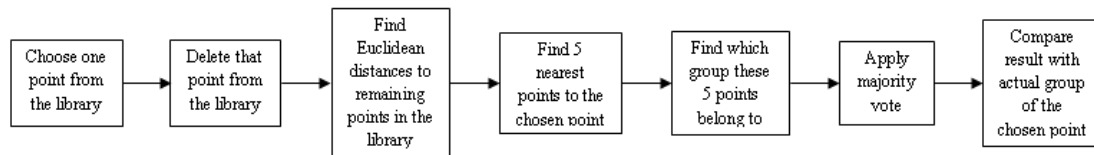


Figure 3.14. Validation of k -NN classifier with “Leave One Out” method on the library

Euclidean distance between two points is calculated as follows.

If $x=(x_1, x_2, x_3, x_4)$ and $y=(y_1, y_2, y_3, y_4)$ are two points in Euclidean 4-space. Then Euclidean distance between x and y , d , is calculated as follows:

$$d = \sqrt{(x_1 - y_1)^2 + (x_2 - y_2)^2 + (x_3 - y_3)^2 + (x_4 - y_4)^2} \quad (3.5)$$

Figure 3.14 shows how k -NN classification works. In the figure, the new test sample, red circle, is to be determined as to whether it belongs to yellow triangles or blue squares. Since, $k=5$ is selected, the test sample belongs to blue squares group.

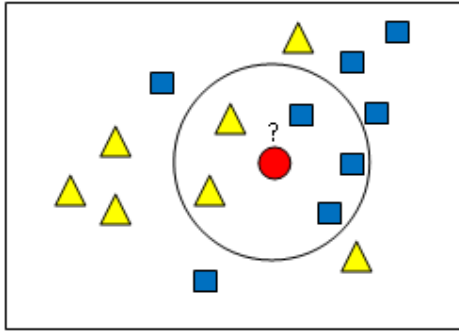


Figure 3.15. Graphical illustration of k-NN classification with k=5

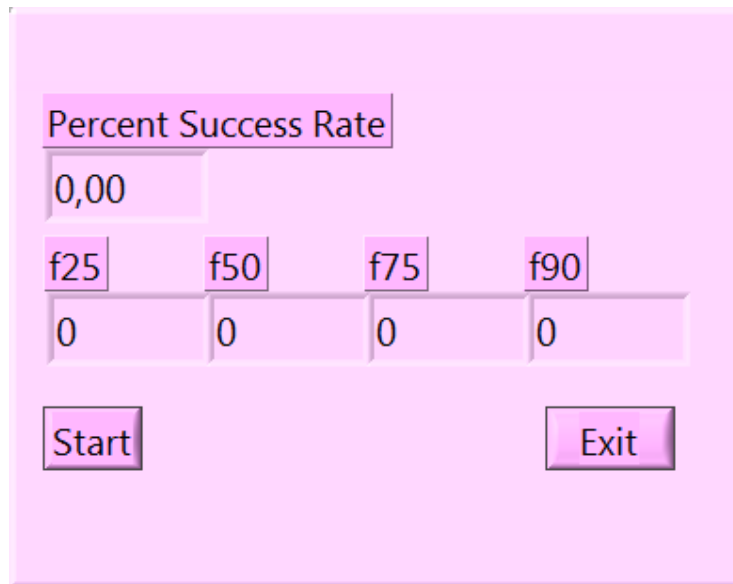


Figure 3.16. User interface of LabVIEW program that calculates the percentage success rate of the library

When “Start” button is pressed, it takes four text documents that contain quartile frequency values of 16 subjects half of which are healthy and half of which are pathological. Then the program chooses one point from the library and calculates Euclidean distances to remaining points in the library. Afterwards, the program determines 7 nearest points to the chosen point and makes a decision by majority vote. This decision is compared with actual class of the point and percentage success rate of all points in the library is calculated and shown on the screen.

Selecting different values for window size, overlap percentage of consecutive windows, k value, and averaging number will affect percentage success rate of the system. There is no consensus in the literature about effect of those parameters to the overall success rate of k-NN classification. Effect of changing averaging number has been already mentioned in Table 3.1. To find optimum values for other parameters, similar tests have been conducted on other parameters also. Table 3.2 shows success rates of k-NN classification of the library for various window sizes.

Table 3.2. k-NN classification success rates of the library for various window sizes for k=5, 25 percent overlap

Window Size	Averaging	Success Rate
1024	10	70.12%
2048	10	76.87%
4096	10	65.62%

Table 3.3 shows k-NN classification success rates of the library for various k and overlap values. Combining all results gives optimum results for averaging number, window size, and overlap percentage of consecutive windows. More clearly, best performance is reached when Averaging=15, Overlap=25 percent, and Window Size=2048. When these values are selected, success rates are very similar for k=3, 5, and 7. k=7 is selected since it gives highest online results rates which will be mentioned in more detail in “Results and Conclusion” part.

Table 3.3. k-NN classification success rates of the library for various k and overlap values

Window Size	k	Overlap	Averaging	Success Rate
2048	5	50	15	71,67
2048	7	50	15	73,96
2048	9	50	15	73,75
2048	3	25	15	77,50
2048	5	25	15	77,50
2048	7	25	15	75,62
2048	3	20	15	74,01
2048	5	20	15	74,30
2048	7	20	15	74,01
2048	9	20	15	73,68
2048	3	30	15	69,64
2048	5	30	15	68,15
2048	7	30	15	68,45

3.6. Analysis

Pressing “Analyze” button prompts a saved record file in “.dat” format. Then, the record, which is expected to be composed of 32000 samples and be sampled at 4000 Hz, is divided into 20 windows of size 2048. Afterwards, for each window, quartile frequencies are calculated. At this point, since there are 20 windows, a vector of size 20 in four dimensions is created which is now ready to be compared with the library to make a decision. Next, k-NN classification is applied using Euclidean distance method with k=7. More clearly, one point is selected from this vector and Euclidean distances to each points in the library are calculated. 7 closest points to the selected point are calculated and majority vote is applied. After this procedure is applied for all 20 points, each point in this vector is classified as healthy or diseased. If 10 or more points are classified as healthy among 20 points, the subject is classified as healthy and the green led flashes.

4. RESULTS

Test results consist of 2 parts, offline and online results. Offline results test the library created to compare online records of new subjects. It uses “Leave One Out” method, which gives one sample in the library to the system to see if the system is able to find the correct result for the given sample. This test will give a percentage of correctness of the system.

Online results part shows results of the system to the real subject records. 12 records are given to the system, 6 of which are of healthy subjects and 6 of which are of pathological subjects. This set is different from the set which is used to create the library.

Window size, averaging number, and overlap percentage of consecutive windows have been decided before. Moreover, for different k and overlap values, online and offline (accuracy) results are measured as shown in table 4.1. Best rates for both online and offline results are measured for k=7 and 25 percent overlap.

Table 4.1. Offline and online results for different “k” and “overlap” values for “window size=2048” and “averaging=15”

k	overlap	offline	online
5	50	71,67	66,11
7	50	73,96	68,05
9	50	73,75	68,89
3	25	77,50	65,41
5	25	77,50	65,83
7	25	75,62	68,75

To sum up, best rates for both online and offline results are obtained for following values:

- Averaging number=15.
- Window size=2048.
- Overlap percentage of consecutive windows=25.
- k=7.

Results are divided into 3 parts: Sensitivity, specificity and accuracy.

Sensitivity is defined as follows:

$$\frac{\textit{Number of samples of pathological subjects classified correctly}}{\textit{Total number of samples of pathological subjects}} \quad (4.1)$$

Specificity is defined as follows:

$$\frac{\textit{Number of samples of healthy subjects classified correctly}}{\textit{Total number of samples of healthy subjects}} \quad (4.2)$$

Accuracy is defined as follows:

$$\frac{\textit{Number of samples classified correctly}}{\textit{Total number of samples}} \quad (4.3)$$

4.1. Offline Results

The library is created with records of 16 subjects, 8 of which are of healthy people and 8 of which are of pathological. Since each record is divided into 20 windows of size 2048 samples, there are 20 points for each record which consist of quartile frequencies. Number of correctly classified samples among these 20 samples is measured. Table 4.1 shows results of 16 records which forms the library of the system.

Table 4.2. Offline results

Record Number	Medical Assessment	Samples	Correctly Classified Samples
1	Healthy	20	18
2	Healthy	20	17
3	Healthy	20	18
4	Healthy	20	16
5	Healthy	20	18
6	Healthy	20	19
7	Healthy	20	13
8	Healthy	20	16
9	Diseased	20	15
10	Diseased	20	16
11	Diseased	20	9
12	Diseased	20	17
13	Diseased	20	19
14	Diseased	20	13
15	Diseased	20	6
16	Diseased	20	12

According to these values, sensitivity is 67 percent($100 \times 107/160$), specificity is 84 percent($100 \times 135/160$), and accuracy is 76 percent($100 \times 242/320$).

4.2. Online Results

Online results are obtained with records of 12 subjects, 6 of which are of healthy people and 6 of which are of pathological. Since each record is divided into 20 windows of size 2048 samples, there are 20 points for each record which consist of quartile frequencies. Number of correctly classified samples among these 20 samples is measured. Table 4.2 shows results of 12 records.

Table 4.3. Online results

Record Number	Medical Assessment	Samples	Correctly Classified Samples
1	Healthy	20	16
2	Healthy	20	17
3	Healthy	20	12
4	Healthy	20	16
5	Healthy	20	11
6	Healthy	20	13
7	Diseased	20	17
8	Diseased	20	14
9	Diseased	20	19
10	Diseased	20	8
11	Diseased	20	15
12	Diseased	20	7

According to these values, sensitivity is 67 percent($100 \times 80/120$), specificity is 71 percent($100 \times 85/120$), and accuracy is 69 percent($100 \times 165/240$).

5. CONCLUSION

In this work, a hand-held device and an adapter unit that is capable of acquisition, filtering, amplification, digitization and processing of respiratory sounds are designed. The adapter unit is responsible for data acquisition, filtering and amplification, whereas the hand-held device is responsible for data digitization and signal processing.

The adapter unit captures respiratory sounds via an electret microphone with an air capsule. And then it filters respiratory data to 80-2000 Hz band. Finally, it amplifies respiratory data, since they are small in magnitude. The adapter unit consumes 193-273 mW which is very low.

The hand-held device first digitizes respiratory data coming from the adapter unit via a DAQ card placed on it. Afterwards, via a user interface program written in LabVIEW, it is capable of recording, plotting, and analyzing respiratory data. Analysis of respiratory data includes making a decision whether the subject is healthy or pathological.

The success rate of all system is tested and calculated to be 76 percent (offline results) and 69 percent (online results). The online and offline success rates seem to be a little bit low. There may be several factors that decrease the success rate of the system. Firstly, the scarcity of recorded respiratory data to train and validate the system may be a significant factor that decreases success rate of the system. Since there were no adequate recorded data, "Leave One Out" algorithm is applied to the library. If there were enough data, a different set of data would be used to validate the library. Moreover, expiration and inspiration phases of respiratory data are not determined after being captured. Therefore, some valuable information may be lost because of this and this will definitely decrease the success rate of the system.

This work demonstrates that a hand-held device that is capable of capturing and analyzing respiratory data is doable. With a more powerful algorithm, this device may be a

valuable and useful tool in medicine. It may replace analog stethoscopes which are most commonly used devices of physicians.

6. FUTURE WORK RECOMMENDATIONS

Some changes on hardware part will definitely improve the overall system. First of all, the memory (RAM) of the PDA is not enough to process large pieces of data. Lack of memory of PDA prevents real time illustration of respiratory sounds. With a PDA which has more memory (RAM), real time illustration of respiratory sounds would be possible and the user interface program would be executed more quickly. Moreover, if SMD equipment is used when building the adapter unit, the volume of the adapter unit would be much smaller, allowing the equipment to be hand-held. Also, if appropriate ICs are selected, the entire adapter unit may be powered from PDA through the DAQ card slot. Therefore, the whole system would be battery-operated.

The algorithm that is used to classify the subjects may be improved also. The algorithm used in the work, does not separate expiration and inspiration phases of respiratory sounds. If respiratory sounds can be separated into expiration and inspiration phases, the success rate of the system would definitely be increased.

APPENDIX A: TECHNICAL DRAWING OF THE MICROPHONE CAPSULE

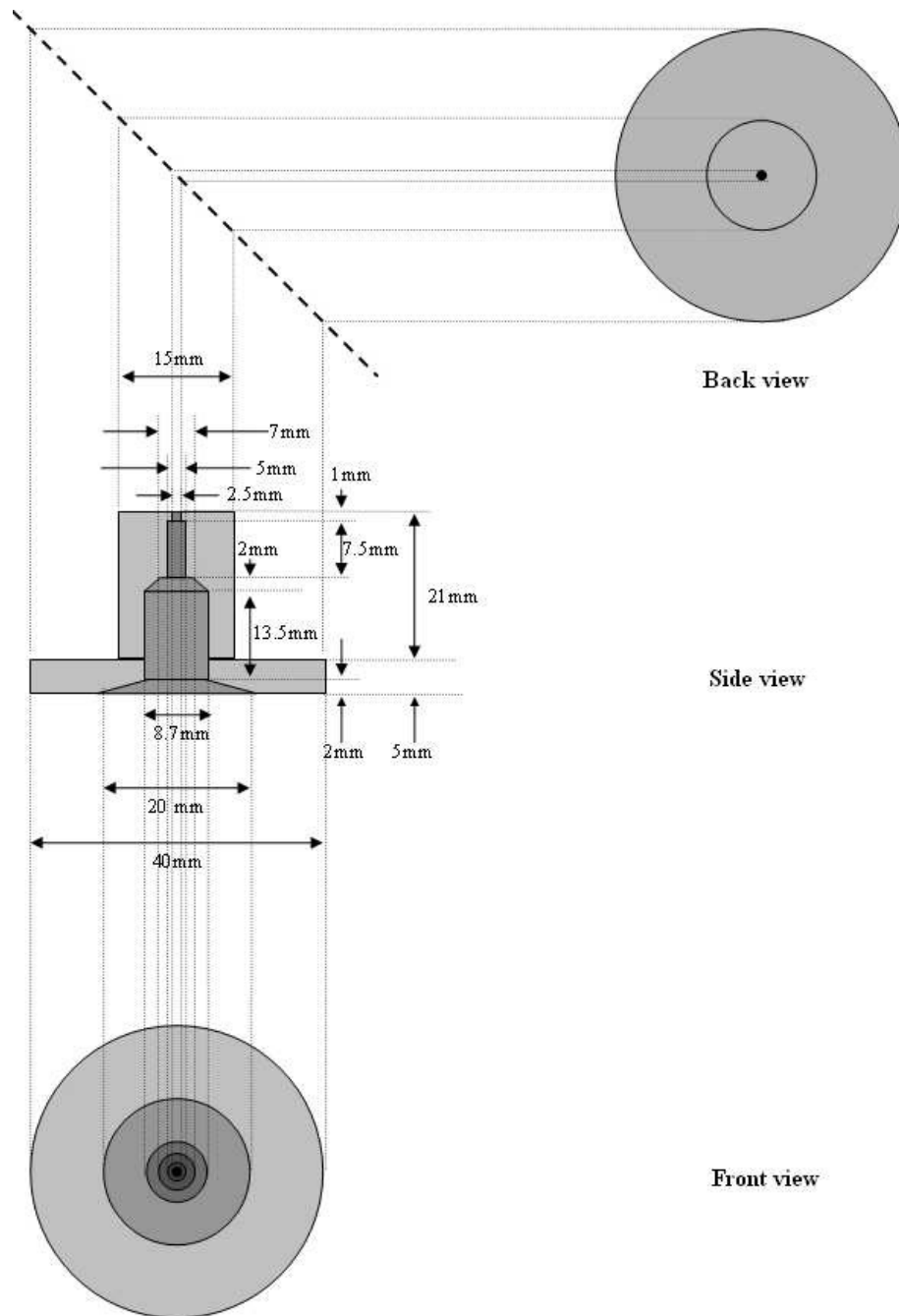
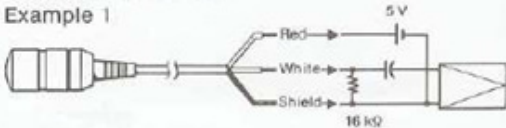
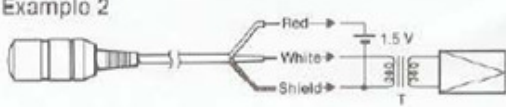


Figure A.1. Technical drawing of the microphone capsules [5]

APPENDIX B: MICROPHONE SPECIFICATIONS

<p style="text-align: center; font-size: 1.2em; font-weight: bold;">SONY</p> <p style="text-align: center; font-size: 0.8em;">ELECTRET CONDENSER MICROPHONE</p> <p style="text-align: center; font-size: 1.5em; font-weight: bold;">ECM-44SPT ECM-44BPT</p> <hr/> <p style="text-align: center; font-weight: bold;">INSTRUCTIONS</p> <p>The Sony ECM-44SPT/44BPT is a miniature-sized, high performance, high reliability professional use microphone, designed for use with a transmitter as part of a wireless microphone system.</p> <p style="text-align: center; font-weight: bold;">MODE D'EMPLOI</p> <p>Le Sony ECM-44SPT/44BPT est un microphone miniature à usage professionnel, très fiable et de haute performance conçu pour être utilisé avec l'émetteur d'un système de microphone sans fil.</p> <p style="text-align: center; font-weight: bold;">ANLEITUNG</p> <p>Das Sony ECM-44SPT/44BPT ist ein Miniatur-Mikrofon hoher Leistung und hoher Zuverlässigkeit für professionelle Anwendung, das speziell für Sender aus dem Drahtlos-Mikrofon-Programm bestimmt ist.</p>	<p style="text-align: center; font-size: 0.8em;">English</p> <p style="text-align: center; font-weight: bold;">SPECIFICATIONS</p> <p>Performance (measured in "Connection Example 1" below)</p> <p>Frequency range 40 to 15,000 Hz</p> <p>Directivity Omni-directional</p> <p>Sensitivity -40.0 dB (10 mV/1 Pa (10 μbar) at 1 kHz Deviation ±3.0 dB</p> <p>Power requirements</p> <p>Supply voltage range: 5.0 to 10.0 V DC (Example 1) 1.1 to 10.0 V DC (Example 2)</p> <p>Current drain: Less than 0.3 mA</p> <p>Noise level</p> <p>Inherent noise: Less than 32 dB SPL (0 dB = 20 μPa)</p> <p>Wind noise: Less than 40 dB SPL (0 dB = 20 μPa) with wind screen</p> <p>General</p> <p>Operating temperature 0°C to 60°C</p> <p>Dimensions 8.5 mm (11/32 in.) dia., 14.5 mm (9/16 in.) long</p> <p>Microphone cable 2.3 mm (7/32 in.) dia., 3 m (10 ft.) long 2-conductor shielded cable (pig tail)</p> <p>Weight Approx. 2 g (0.07 oz) (without cable)</p> <p>Finish ECM-44BPT: Mat black finish ECM-44SPT: Non-reflective satin nickel finish</p> <p>Supplied accessories</p> <p>Wind screen 1 Holder clip 1</p> <p>Design and specifications subject to change without notice.</p> <p style="text-align: center; font-weight: bold;">CONNECTION</p> <p>Example 1</p>  <p>Example 2</p> 
--	--

© 1985 by Sony Corporation

Figure B.1. Microphone specifications [5]

APPENDIX C: DAQ CARD SPECIFICATIONS

Digital logic levels

Level	Min	Max	Units
Input low voltage	-0.3	0.8	V
Input high voltage	2	3.9	V
Input leakage current	-1	1	μ A
Output low voltage (I = 2 mA)	—	0.8	V
Output high voltage (I = 2 mA)	2.5	—	V
Input current (0 < Vin < 3.3 V)	-1	1	μ A

External Voltage References

+3.3 V output (10 mA maximum) 3.3 V typical, 2.97 V minimum

Power Requirements

+3.3 V from PDA host

Idle maximum 2 mA

Typical (continuous acquisition) 50 mA

Maximum (all outputs loaded)..... 68 mA

Physical Characteristics

Dimensions Type II CompactFlash Card

I/O connectors 15-pin

Weight 9 g (0.3 oz)

Environmental

The NI CF-6004 device is intended for indoor use only.

Operating temperature

(IEC 60068-2-1 and IEC 60068-2-2) 0 to 40 °C

Operating humidity

(IEC 60068-2-56) 10 to 90% RH, noncondensing

Storage temperature

(IEC 60068-2-1 and IEC 60068-2-2) -20 to 70 °C

Storage humidity

(IEC 60068-2-56) 5 to 90% RH, noncondensing

Figure C.1. Specifications of DAQ card

Table C.1. Terminal Assignments

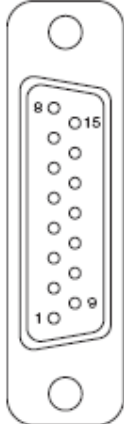
Module	Terminal	Signal	Wire Color
	1	AI GND	White or Red
	2	AI 0	White/Black
	3	AI 1	Red/Black
	4	AI 2	Yellow/Black
	5	AI 3	Green/Black
	6	RSRVD	Green or Blue
	7	RSRVD	Blue/Black
	8	+3.3 V	Brown/White
	9	NC	—
	10	D GND	Orange or Gray
	11	PFI 0	Orange/Black
	12	PFI 1	Gray/Black
	13	PFI 2	Purple/White
	14	PFI 3	Pink/Black
	15	D GND	Purple or Pink

Table C.2. Signal Descriptions

Signal Name	Reference	Direction	Description
AI GND	—	—	Analog Ground —These terminals are the reference point for single-ended AI measurements. The AI GND and D GND ground references are connected on the device.
AI <0..3>	AI GND	Input	Analog Input Channels 0 to 3 —For single-ended measurements, each signal is an analog input voltage channel.
+3.3 V	D GND	Output	+3.3 V Power Source —Provides +3.3 V power up to 10 mA.
D GND	—	—	Digital Ground —D GND supplies the reference for PFI <0..3> and +3.3 V. The AI GND and D GND ground references are connected on the device.
PFI <0..3>	D GND	Input or Output	Programmable Function I/O or Digital I/O —Each of these terminals are configurable as a PFI terminal or a digital I/O terminal. You can individually configure each digital I/O signal as an input or output. You can configure any of the terminals as a PFI input for a digital AI trigger.

REFERENCES

1. P. D. Welsby, G. Parry, D. Smith, "The Stethoscope: Some Preliminary Investigations", *Postgrad Medicine*, Vol. 79, pp. 695–698, June 2003.
2. Pasterkamp H., S. S. Kraman and G. R. Wodicka, "Advances Beyond the Stethoscope", *American Journal of Respiratory and Critical Care Medicine*, Vol. 156, pp.974-987, September 1997.
3. Sergül Aydıre, "Wheeze Detection in Respiratory Sounds via Statistical Signal Modelling", Boğaziçi University Master of Science Thesis, 2009.
4. Gavriely N., *Breath Sounds Methodology*, CRC Press, Boca Raton, FL, 1995.
5. Earis J. E. and B. M. G. Cheetham, "Current Methods Used for Computerized Respiratory Sound Analysis", *European Respiratory Review*, Vol. 10, No.77, pp. 586-590, 2000.
6. İpek Şen, "A Multi-Channel Device for Respiratory Sound Data Acquisition and Transient
7. Omar Alghamdi, "Computerized Lung Sounds Analysis using LabVIEW"
8. Detection", Boğaziçi University Master of Science Thesis, 2005.
9. Franco S., *Design with Operational Amplifiers and Analog Integrated Circuits*, 3rd Ed., McGraw-Hill, 2002.
10. Kraman S. S., G. R. Wodicka, Y. Oh and H. Pasterkamp, "Measurement of Respiratory Acoustic Signals - Effect of Microphone Air Cavity Width, Shape, and Venting", *Chest*, Vol. 108, pp. 1004-1008, 1995.
11. Vanuccini L., J. E. Earis, P. Helisto, B. M. G. Cheetham, M. Rossi, A. R. A. Sovijarvi and J. Vanderschoot, "Capturing and Preprocessing of Respiratory Sounds", *European Respiratory Review*, Vol. 10, No. 77, pp. 616-620, 2000.
12. Stoica P., Moses R. L., *Introduction to Spectral Analysis*, Prentice Hall, 2005.